Blind Adaptive Spatial Processing in a Mobile Radio Environment*

Jeffrey L. Schenck and William A. Gardner
Department of Electrical and Computer Engineering
University of California, Davis
Davis, CA 95616

Abstract

In this paper, we use blind adaptive spatial filtering to extract spectrally overlapping FM cellular radio signals. The technique presented here uses a programmable transformation to derive a training signal from the received data. Simulation results show that a variety of transformations are capable of producing high-quality signal estimates. A transformation producing a structure similar to the Cross-SCORE algorithm may be useful for exploiting the cyclostationarity introduced by the supervisory audio tone present in the baseband of the analog FM signal. The issue of convergence behavior is also discussed.

I Introduction

As the demand for cellular communication services continues to grow, system resources must be used more efficiently. Current efforts to increase the number of users primarily focus on digital techniques (e.g., CDMA). Another approach to increasing the number of users in a mobile radio environment is to employ spatial processing. This would allow separation of spectrally overlapping signals through the use of space-division multiplexing. Such an approach is presented in [1], where the SCORE algorithm [2] adapts a sensor array by exploiting spectral correlation in PSK signals.

In order to expand the capacity of the U.S. Advanced Mobile Phone System (AMPS) by means of spatial processing, the absence of a training signal, as well as an unknown (and changing) direction of arrival (DOA), implies the need for a blind adaptive spatial filter. The technique presented here, Programmable Canonical Correlation Analysis (PCCA), is a flexible and robust algorithm for blindly adapting antenna arrays. Knowledge of array calibration data and signal DOA is not required. A training signal is generated locally from the received data using a programmable reference-path transformation. An appropriate transformation is chosen based on the signal environment. A wide variety of transformations are potentially useful [3, 4, 5], only a few of which are presented here.

Section II describes the AMPS signal format and the assumed environment model. The PCCA algorithm and some of its variants are discussed in Section III. Simulation results using actual AMPS data collects are presented in Section IV.

II Signal Environment

In the AMPS system, voice is transmitted by frequency modulating an RF carrier in the 800–900 MHz. band. Transmission and reception occur in different frequency bands. Neighboring cells operate in different frequency bands so as to avoid interference between cells.

The FM voice signal baseband contains an audio signal that has been bandlimited to 3000 Hz. and filtered with a pre-emphasis filter. The baseband also contains a supervisory audio tone (SAT) at approximately 6 kHz. This composite signal is frequency modulated with a deviation of 12 kHz. to produce a signal bandwidth of roughly 30 kHz.

The signals used in the computer simulations described here are all collected off-the-air, sampled, down-converted, and filtered in order to form their complex envelope representations. The signals are combined with white Gaussian noise, simulating an environment containing spectrally overlapping but frequency-offset signals.

We assume a two-dimensional array geometry throughout this paper and that a narrowband signal model is appropriate. The sensor array output can be written as

$$\boldsymbol{x}(t) = \boldsymbol{A}(\boldsymbol{\theta})\boldsymbol{s}(t) + \boldsymbol{n}(t),$$

where the vector $\boldsymbol{s}(t)$ contains L uncorrelated AMPS signals, $\boldsymbol{A}(\boldsymbol{\theta})$ is the $M \times L$ array response matrix, $\boldsymbol{\theta}$

*This work was supported in part by the Office of Naval Research under contract N00014-92-J-1218.

is the signal DOA vector, and $n(t)$ is an $M \times 1$ vector of spatially white noise.

III PCCA

Canonical correlation analysis (CCA) was developed by Hotelling [6] in the 1930's as a way of relating two sets of random variables. Here we describe this technique and how it can be applied to antenna arrays.

III.A CCA

Suppose we have two random vectors, $\boldsymbol{x}(t)$ and $\boldsymbol{y}(t)$, whose empirical correlation matrix is defined as

$$\boldsymbol{R}_{\mathbf{xy}} \triangleq \langle \boldsymbol{x}(t)\boldsymbol{y}^H(t)\rangle .$$

Let us define two random variables $u_1(t) = \boldsymbol{a}_1^H\boldsymbol{x}(t)$ and $v_1(t) = \boldsymbol{b}_1^H\boldsymbol{y}(t)$. We want to choose $\boldsymbol{a}_1$ and $\boldsymbol{b}_1$ so that the magnitude of the correlation between $u_1(t)$ and $v_1(t)$ is maximized. These are the *first pair of canonical variables.* We then define the *second pair of canonical variables* as the linear combinations $u_2(t) = \boldsymbol{a}_2^H\boldsymbol{x}(t)$ and $v_2(t) = \boldsymbol{b}_2^H\boldsymbol{y}(t)$ that are maximally correlated with each other and constrained to be uncorrelated with the first pair of canonical variables. Similarly, the k*th pair of canonical variables* are the linear combinations that are maximally correlated among all variables uncorrelated with the previous $k-1$ pairs. The correlation between the kth pair of canonical variables is called the k*th canonical correlation.* We now have two vectors, $\boldsymbol{u}(t)$ and $\boldsymbol{v}(t)$, that consist of ordered pairs of variables that are maximally correlated with each other but uncorrelated with all other elements of the vectors.

The coefficient vectors $\boldsymbol{a}_k$ and $\boldsymbol{b}_k$ are given by the following eigenequations (cf. [7]):

$$\boldsymbol{R}_{\mathbf{xx}}^{-1}\boldsymbol{R}_{\mathbf{xy}}\boldsymbol{R}_{\mathbf{yy}}^{-1}\boldsymbol{R}_{\mathbf{yx}}\boldsymbol{a}_k = \lambda_k \boldsymbol{a}_k$$

$$\boldsymbol{R}_{\mathbf{yy}}^{-1}\boldsymbol{R}_{\mathbf{yx}}\boldsymbol{R}_{\mathbf{xx}}^{-1}\boldsymbol{R}_{\mathbf{xy}}\boldsymbol{b}_k = \lambda_k \boldsymbol{b}_k,$$

where λ_k is the kth-largest eigenvalue and is equal to the squared magnitude of the correlation coefficient of $u_k(t)$ and $v_k(t)$. The canonical variates have the properties

$$E\{u_i u_i^*\} = E\{v_i v_i^*\} = 1$$

$$E\{u_i v_i^*\} = \rho_i$$

$$E\{u_i v_j^*\} = E\{u_i u_j^*\} = E\{v_i v_j^*\} = 0, \qquad i \neq j,$$

where ρ_i is the correlation coefficient of $u_i(t)$ and $v_i(t)$. Note that the vectors $\boldsymbol{a}_k$ and $\boldsymbol{b}_k$ are unique unless two or more pairs of canonical variables have the same correlation magnitude, i.e., if $|\lambda_k| = |\lambda_{k+1}|$.

III.B CCA Applied to Sensor Arrays

The theory of canonical correlation is applied to adaptive antenna arrays in [5, 4, 3]. Here we review this approach. Let $\boldsymbol{x}(t)$ be the output of an N-element antenna array and $\boldsymbol{y}(t)$ be the output of a user-programmable transformation of $\boldsymbol{x}(t)$. In general, the transformation is chosen to decorrelate components belonging to signals of no interest (SONI's) in $\boldsymbol{x}(t)$ and $\boldsymbol{y}(t)$ while maintaining a high distinct correlation between signal of interest (SOI) components. CCA is then applied to $\boldsymbol{x}(t)$ and $\boldsymbol{y}(t)$ to produce the eigenequations

$$\boldsymbol{R}_{\mathbf{xx}}^{-1}\boldsymbol{R}_{\mathbf{xy}}\boldsymbol{R}_{\mathbf{yy}}^{-1}\boldsymbol{R}_{\mathbf{yx}}\boldsymbol{W}_x = \boldsymbol{W}_x\boldsymbol{\Lambda}$$

$$\boldsymbol{R}_{\mathbf{yy}}^{-1}\boldsymbol{R}_{\mathbf{yx}}\boldsymbol{R}_{\mathbf{xx}}^{-1}\boldsymbol{R}_{\mathbf{xy}}\boldsymbol{W}_y = \boldsymbol{W}_y\boldsymbol{\Lambda}.$$

The eigenvectors are used as spatial filter weights to produce canonical variates denoted by $\hat{\boldsymbol{s}}(t)$ and $\hat{\boldsymbol{d}}(t)$:

$$\hat{\boldsymbol{s}}(t) = \boldsymbol{W}_x^H\boldsymbol{x}(t)$$

$$\hat{\boldsymbol{d}}(t) = \boldsymbol{W}_y^H\boldsymbol{y}(t)$$

A block diagram of the PCCA algorithm is shown in Figure 1.

If the reference-path transformation is able to decorrelate the SONI's while retaining sufficient correlation between SOI components in $\boldsymbol{x}(t)$ and $\boldsymbol{y}(t)$, the first canonical variable, $\hat{s}_1(t)$, can be a high-quality estimate of the SOI. Note that the training signal $\hat{d}_1(t)$ need not be a high-quality estimate; it only needs to be sufficiently correlated with $\hat{s}_1(t)$. In fact, each of the elements of $\hat{\boldsymbol{s}}(t)$ can be a signal estimate. It is shown in [4] that if the elements of $\boldsymbol{s}(t)$ are uncorrelated and the resulting canonical correlation magnitudes are distinct, then the PCCA signal estimates are comparable in quality to those produced by the minimum mean square error beamformer. Thus, in some environments, where the reference-path transformation is chosen judiciously, multiple signals can be extracted by using each signal's corresponding eigenvector as a set of array weights.

III.C Transformations

As mentioned, the reference-path transformation should be chosen so that the correlations between signal components in data vectors $\boldsymbol{x}(t)$ and $\boldsymbol{y}(t)$ have different magnitudes. Possible transformations include:

- $\boldsymbol{y}(t)$ is a frequency-shifted (by α) and delayed (by τ) version of $\boldsymbol{x}(t)$ or $\boldsymbol{x}^*(t)$, which is equivalent to the Cross-SCORE algorithm. This can be generalized to multiple values of α and τ in order to improve convergence behavior.

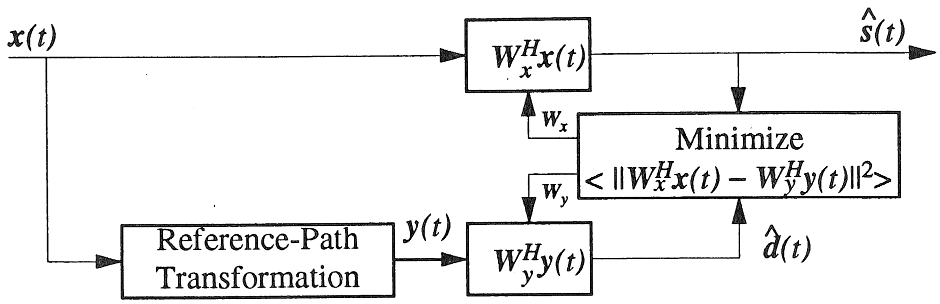

Figure 1: Block diagram of PCCA.

- $y(t)$ is the output of a bandpass or bandstop filter, allowing separation of signals with possibly overlapping spectra, but with different regions of support.
- $y(t)$ is a delayed version of $x(t)$, allowing separation of signals with differing coherence times (or bandwidths). It is shown in [4] that a delay transformation can also be used to mitigate the effects of multipath.
- $y(t)$ is the output of a time-gating operation, where either the SOI or SONI has a duty cycle of less than 100%.
- $y(t)$ is the output of a modulus restoration filter for cases where the SOI has a constant envelope.

III.D PCCA Variants

Phase-PCCA. For some applications, we would like to separate signals based on differences in their correlation phases instead of, or in addition to, their magnitudes. A modification of PCCA called Phase-PCCA (or φ-PCCA) has this capability. Although φ-PCCA is not known to be the solution to an optimization problem, it has been very effective in computer simulations.

φ-PCCA is similar in form to Phase-SCORE [8]. The algorithm structure is the same as that shown in Figure 1, except that the weight vectors are solutions to a different eigenequation:

$$\boldsymbol{R}_{\mathbf{xx}}^{-1}\boldsymbol{R}_{\mathbf{xy}}\boldsymbol{W}_x = \boldsymbol{W}_x\boldsymbol{\Lambda}.$$

Reduced-Rank PCCA. Solving the PCCA and φ-PCCA eigenequations involves inverting correlation matrices. Ideally, these matrices are not singular. Matrices estimated from finite data collects, however, may be poorly conditioned for small collect times. Thus, perturbations in the small eigenvalues of $\boldsymbol{R}_{\mathbf{xx}}$ produce large errors in $\boldsymbol{R}_{\mathbf{xx}}^{-1}$. The effects of this problem can be reduced by replacing $\boldsymbol{R}_{\mathbf{xx}}^{-1}$ with its pseudoinverse

$$\boldsymbol{R}_{\mathbf{xx}}^{+} \triangleq \sum_{l=1}^{L_x} \frac{1}{\lambda_l} \boldsymbol{e}_l \boldsymbol{e}_l^H,$$

where L_x is the rank of $\boldsymbol{R}_{\mathbf{xx}}$, λ_l is its lth eigenvalue, and $\boldsymbol{e}_l$ is its lth eigenvector.

In [9], Biedka replaces the matrix inverses with pseudoinverses in the SCORE eigenequations to obtain what he calls Subspace-Constrained SCORE. Similarly, substituting pseudoinverses into the PCCA equation produces Reduced-Rank PCCA (RR-PCCA) and is described by the eigenequations

$$\boldsymbol{R}_{\mathbf{xx}}^{+}\boldsymbol{R}_{\mathbf{xy}}\boldsymbol{R}_{\mathbf{yy}}^{+}\boldsymbol{R}_{\mathbf{yx}}\boldsymbol{W}_x = \boldsymbol{W}_x\boldsymbol{\Lambda}$$

$$\boldsymbol{R}_{\mathbf{yy}}^{+}\boldsymbol{R}_{\mathbf{yx}}\boldsymbol{R}_{\mathbf{xx}}^{+}\boldsymbol{R}_{\mathbf{xy}}\boldsymbol{W}_y = \boldsymbol{W}_y\boldsymbol{\Lambda}.$$

A similar substitution produces a reduced-rank version of φ-PCCA. Simulation results in Section IV demonstrate improved convergence behavior for this technique over plain PCCA.

IV Simulation Results

Here we present results obtained with PCCA and its relatives using environments generated from live AMPS data described in Section II. The environments contain spectrally overlapping but frequency-offset signals, which is a modification of the existing AMPS system. In each experiment, correlation matrices are created from the available data. The output signal-to-interference and noise ratios (SINR's) of resulting SOI estimates are averaged to produce a mean SINR for each collect time.

IV.A CMA

An environment containing four AMPS signals is received by a five-element linear array with half-wavelength spacing and is described in Table 1. A temporal least-squares CMA algorithm [10] is used as the reference-path transformation. It adapts an

Signal	f_c (kHz)	AOA	In-band SNR (dB) Env. 1	Env. 2
SOI	0	10	18	18
SONI1	-10	-20	13	11
SONI2	5	30	12	10
SONI3	15	45	15	12

Table 1: Simulation parameters for sparse AMPS environments.

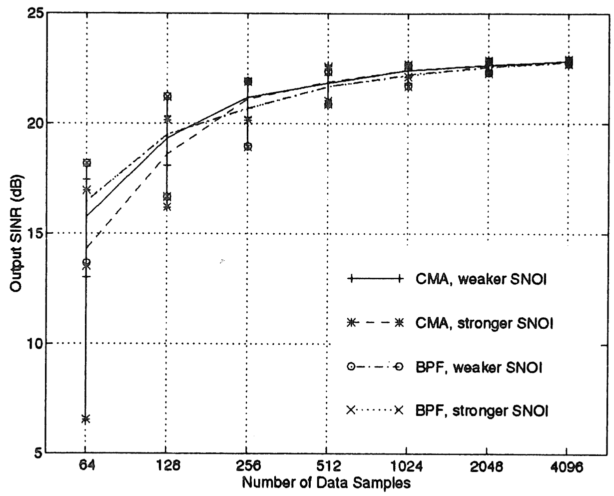

Figure 2: Average output SINR for AMPS cellular radio signals using CMA and bandpass filter reference-path transformations. Error bars indicate one standard deviation in each direction over 10 trials.

Signal	f_c (kHz)	AOA	In-band SNR (dB) Env. 1	Env. 2
SOI	0	10	18	18
SONI 1	-15	-65	12	10
SONI 2	-10	30	15	12
SONI 3	-5	-40	13	11
SONI 4	5	-20	12	10
SONI 5	10	70	13	11
SONI 6	15	45	15	12

Table 2: Simulation parameters for dense AMPS environments.

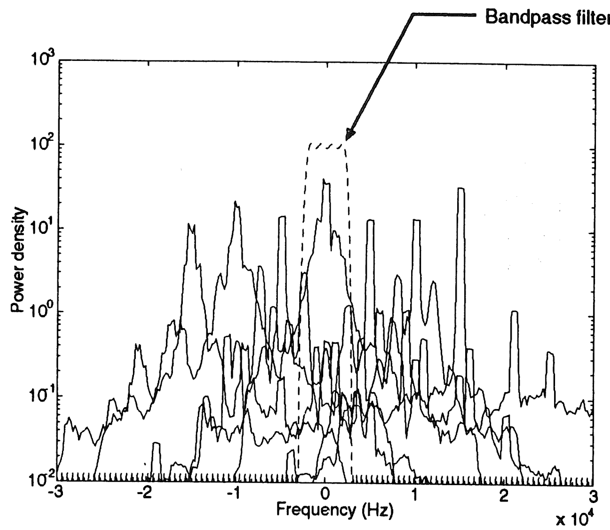

Figure 3: Spectra of individual AMPS signals in dense environment. Bandpass filter transformation is also shown. Noise spectrum is not shown.

eight-tap FIR filter enforcing a constant modulus cost function. Since the SOI is the strongest signal in the environment, the CMA captures it and suppresses the SONI's. Although the CMA distorts the SOI in the reference path, its output is still useful as a training signal. Figure 2 plots the output SINR versus collect time for both environments. PCCA is able to extract a high-quality SOI estimate.

Also plotted in Figure 2 are SINR results for experiments using a 10 kHz. bandpass filter as the reference-path transformation. The results are very similar to those obtained with the CMA. Although the bandpass filter allows the user to specify which signal he wants to extract, CMA is useful for applications where the exact carrier frequency of the SOI is unknown.

IV.B Bandpass Filter

A denser signal environment is described in Table 2 and received by an eight-element linear array. The individual signal spectra are plotted in Figure 3. We see that most of a signal's energy is concentrated near its carrier. Therefore we can use a narrow (5 kHz.) bandpass transformation to isolate the SOI. The average output SINR is plotted in Figure 4. Given enough adaptation time, PCCA produces a high-SINR SOI estimate.

Because of a fade rate of roughly 100 Hz., We would like to be able to produce high-quality signal estimates in much less than 10 msec. In the next section, we modify this experiment in order to improve PCCA convergence behavior.

IV.C RR-PCCA

As mentioned in Section III, if either $\boldsymbol{R}_{\mathbf{xx}}$ or $\boldsymbol{R}_{\mathbf{yy}}$ has small eigenvalues, PCCA performance can be poor for small collect times. Table 3 displays the autocorrelation matrix eigenvalues of the dense envi-

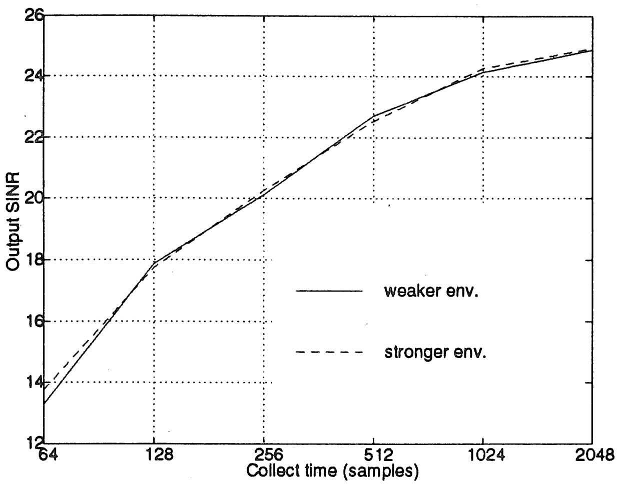

Figure 4: Average output SINR for AMPS SOI using 5 kHz. bandpass filter transformation. Ten trials are run at each collect time. 71 samples = 1 msec.

Env. 1		Env. 2	
$\boldsymbol{R}_{\mathbf{xx}}$	$\boldsymbol{R}_{\mathbf{yy}}$	$\boldsymbol{R}_{\mathbf{xx}}$	$\boldsymbol{R}_{\mathbf{yy}}$
232.46	191.53	225.97	191.71
111.48	5.08	58.27	3.18
92.14	3.32	57.86	2.07
74.71	2.35	43.47	1.26
57.51	0.79	34.11	0.52
49.61	0.67	29.81	0.38
15.77	0.22	9.76	0.17
0.43	0.06	0.43	0.06

Table 3: Eigenvalues of signal path and reference path correlation matrices for the dense AMPS environments.

ronments used in the previous example. We see that $\boldsymbol{R}_{\mathbf{yy}}$ has only one large eigenvalue, whereas $\boldsymbol{R}_{\mathbf{xx}}$ has broadly distributed eigenvalues. Thus we can expect an improvement in performance by using RR-PCCA.

The results of using RR-PCCA on the weaker of the dense AMPS environment are plotted in Figures 5 through 7. The ranks of $\boldsymbol{R}^+_{\mathbf{xx}}$ and $\boldsymbol{R}^+_{\mathbf{yy}}$ range from one to eight. Collect times T range from 64 to 2048 samples. Results for the stronger environment are similar to those plotted except that, for small values of T and $\boldsymbol{R}^+_{\mathbf{xx}}$ rank, SINR results are slightly poorer.

In Figure 5, the collect time is fixed at 64 samples. We see that, for such short collects, the peak performance is at $L_x = 3$ or 4 and $L_y = 1$. $L_y = 1$ produces the best results for all collect times and values of L_x. This is consistent with the fact that $\boldsymbol{R}_{\mathbf{yy}}$ has only

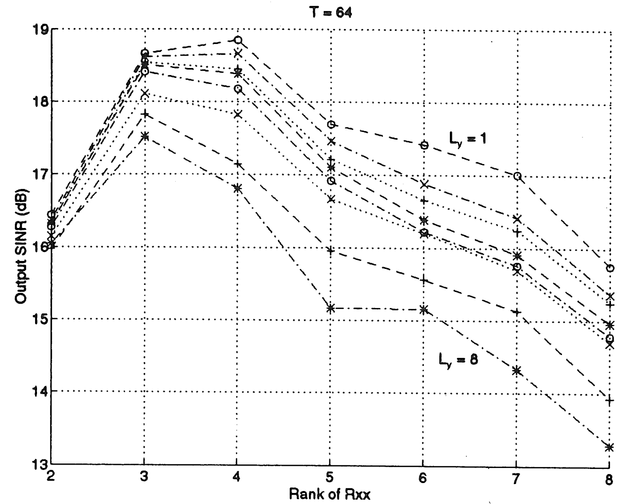

Figure 5: Average output SINR plotted versus rank of $\boldsymbol{R}^+_{\mathbf{xx}}$, $T = 64$ samples. Rank of $\boldsymbol{R}^+_{\mathbf{yy}}$ is the parameter. The best performance is given by $L_y = 1$; $L_y = 8$ gives the poorest. Ten trials are run for each combination of rank values.

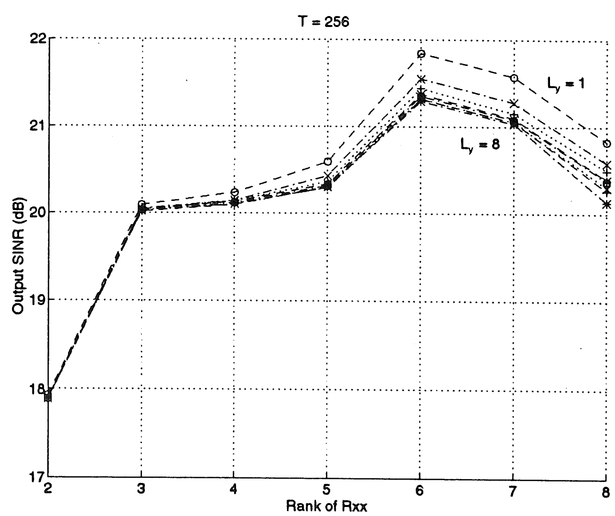

Figure 6: Average output SINR plotted versus rank of $\boldsymbol{R}^+_{\mathbf{xx}}$, $T = 256$ samples. The curves merge completely as collect time increases.

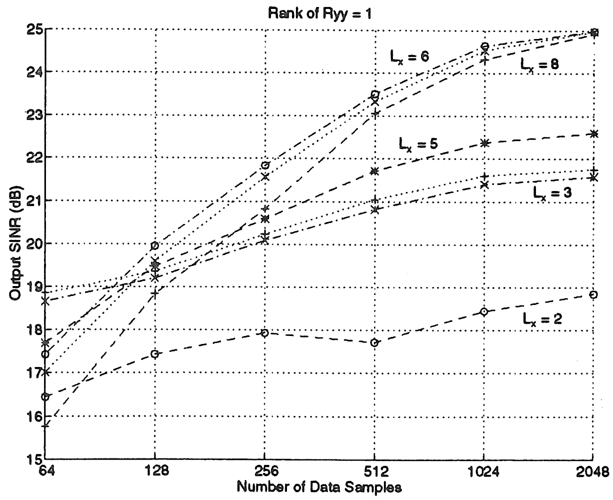

Figure 7: Average output SINR plotted versus collect time. Rank of $R^+_{\mathbf{xx}}$ is the parameter, ranging from two to eight. Rank of $R^+_{\mathbf{yy}} = 1$. Ten trials are run for each combination of rank and collect time. 71 samples = 1 msec.

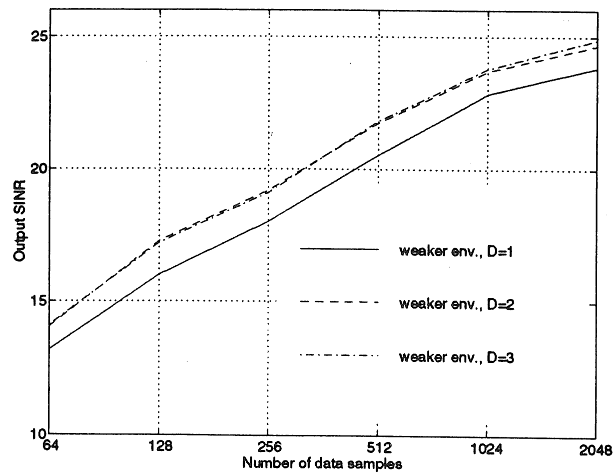

Figure 8: Average output SINR for AMPS cellular radio SOI in weaker of two dense interference environments. φ-PCCA was used with a reference-path delay of $\Delta = 1$, 2, and 3 samples. Ten trials are run. 71 samples = 1 msec.

one large eigenvalue. By choosing $L_y = 1$ and $L_x = 4$, RR-PCCA yields an SINR improvement over plain PCCA of almost 6 dB.

As collect time is increased, the value of L_y has less of an effect on performance, but L_x must be increased to produce the maximum SINR. Thus we see that the optimal rank of $R^+_{\mathbf{yy}}$ is unambiguous and independent of collect time, whereas the optimal rank of $R^+_{\mathbf{xx}}$ is a function of collect time. The performance trade-off between L_x and collect time is presented concisely in Figure 7, where L_y is fixed at one and average output SINR is plotted versus collect time. Each curve represents a different value of L_x. For small collect times, even significantly underestimated values of L_x can produce good results. A value of $L_x = 6$ is optimal for all but the smallest collect time. This is also consistent with the eigenvalue data in Table 3.

IV.D Phase-PCCA

Consider the analytic signal $u(t)$ with carrier frequency f_0:

$$u(t) = s(t)e^{i(2\pi f_0 t + \theta_0)}.$$

Its empirical autocorrelation function is given by

$$R_u(\tau) = \langle u(t+\tau)u(t)^* \rangle$$

$$\begin{aligned} &= \left\langle s(t+\tau)e^{i[2\pi f_0(t+\tau)+\theta_0]}s(t)^* e^{-i(2\pi f_0 t+\theta_0)} \right\rangle \\ &= R_s(\tau)e^{i2\pi f_0 \tau}. \end{aligned}$$

The correlation between $u(t)$ and a delayed version of itself is thus

$$\begin{aligned} \rho_u(\tau) &= \frac{R_u(\tau)}{R_u(0)} \\ &= \rho_s(\tau)e^{i2\pi f_0 \tau}. \end{aligned}$$

Thus for small delays, the phase of a signal's correlation coefficient is proportional to its carrier frequency in radians multiplied by the delay. By placing a small delay in the reference path of φ-PCCA, correlations between components in the two paths will have different phases for each signal. This allows φ-PCCA to separate signals based on differences in their carrier frequencies.

Phase-PCCA with a pure delay is applied to the dense AMPS environments described in Table 2. Output SINR results for the weaker of the two environments are plotted in Figure 8 for delays of one, two, and three samples. (Performance in the other environment is virtually identical.) Delays of $\Delta = 2$ and 3 produce roughly 1 dB of improvement in SINR over $\Delta = 1$, probably because of increased separation of correlation coefficients, as measured by the φ-PCCA eigenvalues.

This approach to extracting AMPS signals has the advantage of being able to extract multiple SOI's simultaneously. It's convergence behavior is similar to that of plain PCCA with a bandpass transformation. A reduced-rank version of φ-PCCA may improve performance, but this approach has not yet been tested.

V Conclusions

In this paper, we have demonstrated the effectiveness of applying blind adaptive spatial filtering to cellular radio environments. Here we have focused on a method for expanding system capacity by using spectrally overlapping but frequency-offset analog voice signals and spatially separating the signals at the base station. The PCCA family of algorithms is ideally suited to this application. PCCA can separate signals based on differences in their regions of spectral support, carrier frequencies, or other characteristics.

In cases where AMPS signals are completely spectrally coincident, other approaches may be employed. For example, the presence of the SAT in the signal baseband introduces cyclostationarity. Because each signal's SAT has a unique phase, φ-PCCA may be able to separate the signals since their cyclic correlation coefficients will all have different phases. Although the resulting cyclic feature is weak, PCCA (unlike SCORE) can exploit features at multiple cycle frequencies, possibly improving convergence behavior. Rank-reduced methods may also be helpful in this regard. This approach is currently being explored.

References

[1] W. A. Gardner, S. V. Schell, and P. A. Murphy, "Multiplication of cellular radio capacity by blind adaptive spatial filtering", in *Proceedings of the International Conference on Selected Topics in Wireless Communications*, Vancouver, B.C., Canada, June 1992.

[2] B. G. Agee, S. V. Schell, and W. A. Gardner, "Spectral self-coherence restoral: A new approach to blind adaptive signal extraction using antenna arrays", *Proceedings of the IEEE*, vol. 78, no. 4, pp. 753–767, April 1990.

[3] W. A. Gardner, J. L. Schenck, and S. V. Schell, "Programmable blind adaptive spatial filtering", in *Proceedings of the IEEE International Conference on Acoustics, Speech, and Signal Processing*, Adelaide, Australia, 1994.

[4] S. V. Schell and W. A. Gardner, "Programmable canonical correlation analysis: A flexible framework for blind adaptive spatial filtering", Submitted to *IEEE Transactions on Signal Processing.*

[5] S. V. Schell, "An overview of sensor array processing for cyclostationary signals", in *Cyclostationarity in Communications and Signal Processing*, William A. Gardner, Ed., chapter 3, pp. 168–239. IEEE Press, New York, 1994.

[6] H. Hotelling, "Relations between two sets of variables", *Biometrika*, vol. 28, pp. 321–377, 1936.

[7] R. A. Johnson and D. W. Wichern, *Applied Multivariate Statistical Analysis*, Prentice-Hall, Englewood Cliffs, New Jersey, third edition, 1992.

[8] S. V. Schell and B. G. Agee, "Application of the SCORE algorithm and SCORE extensions to sorting in the rank-L spectral self-coherence environment", in *Proceedings of the Twenty-Second Asilomar Conference on Signals, Systems, and Computers*, Pacific Grove, Ca., November 1988, pp. 274–278.

[9] T. E. Biedka, "Subspace-constrained SCORE algorithms", in *Proceedings of the Twenty-Seventh Asilomar Conference on Signals, Systems, and Computers*, Pacific Grove, Ca., November 1993.

[10] B. G. Agee, "The least-squares CMA: A new technique for rapid correction of constant modulus signals", in *Proceedings of the IEEE International Conference on Acoustics, Speech, and Signal Processing*, Tokyo, Japan, April 1986.